Phosphotransfer between CheA, CheY1, and CheY2 in the Chemotaxis Signal Transduction Chain of *Rhizobium meliloti*†

Victor Sourjik and Rüdiger Schmitt*

Lehrstuhl für Genetik, Universität Regensburg, D-93040 Regensburg, Germany

Received September 18, 1997; Revised Manuscript Received December 2, 1997

ABSTRACT: The soil bacterium *Rhizobium meliloti* responds to chemotactic stimuli by modulating the rotary speed of its flagella. Unlike in *Escherichia coli*, the signal transduction chain of *R. meliloti* contains two different response regulators, CheY1 and CheY2, but no CheZ phosphatase. Phosphorylation of CheY1 and CheY2 by the central ATP-dependent autokinase, CheA, is the crucial step in signal transduction. In vivo, phospho-CheY2 (CheY2-P) is the chief regulator of flagellar rotation, its action being modulated by CheY1 [Sourjik, V., and Schmitt, R. (1996) *Mol. Microbiol. 22*, 427−436]. In this study, we have investigated these phosphotransfer reactions in vitro using the radiolabeled recombinant proteins, CheA (labeled via [γ-^{32}P]ATP), CheY1, and CheY2 (labeled via acetyl [^{32}P]phosphate). Our results are consistent with the following four-step phosphotransfer: (i) ATP-dependent autophosphorylation of CheA (with a limiting rate constant of 0.008 s^{-1} at saturating ATP concentrations); (ii) rapid phospho transfer from phospho-CheA to CheY1 and CheY2; (iii) autodephosphorylation of CheY1-P and CheY2-P with half-lives of 12 ± 1 s and 10.5 ± 1 s, respectively; and (iv) reversible phosphotransfer from CheY2-P to CheA. In the three-component mixture, CheA/CheY1/CheY2, we observed rapid phosphotransfer from CheY2-P via CheA to CheY1. Thus, CheY1 assumes the role of a "phosphatase" of CheY2-P by acting as a sink for phosphate, whenever unphosphorylated CheA is present. The intracellular concentrations of CheA/CheY1/CheY2 determined immunochemically were 1.5 μM:20 μM:20 μM, a range that was adopted for in vitro assays. The results reflect a unique control by CheY1 of the active, phosphorylated state of the main response regulator, CheY2-P. This mechanism appears to be a new twist to signal transduction among members of the α-subgroup of proteobacteria.

Bacteria adapt to changes in external environment by adjusting their behavior and metabolism. Many of these processes are controlled by "two-component" systems (*1*). Central to these systems is a histidine kinase, whose rate of autophosphorylation is regulated by the sensor portion of the protein. Once phosphorylated, the kinase phosphorylates a conserved aspartyl residue of the response regulator. An additional phosphatase activity that mediates dephosphorylation of the response regulator has been found in most two-component systems (*2*).

The *Escherichia coli* chemotaxis system has been most extensively studied genetically and biochemically (*3*−*7*). CheA is a 73-kDa[1] cytoplasmic protein kinase that catalyzes the transfer of the γ-phosphoryl group of ATP to a conserved His-48. CheA autophosphorylation is regulated in vivo by chemotactic stimuli (*8*). P-CheA, in turn, phosphorylates the response regulator, CheY, at a conserved Asp-57 residue (*9*). The phosphorylated form, CheY-P, interacts directly with the flagellar motor to control the 3D-swimming pattern of the bacterial cell (*10*). The level of CheY-P in the cell is controlled not only by the rate of CheY phosphorylation but also by the rate of its dephosphorylation. If denatured by sodium dodecyl sulfate, CheY-P exhibits a half-life of several hours; however, under nondenaturing conditions the half-life is about 20 s (*11*). It has been shown that this autodephosphorylation reaction is independent of CheA but is dramatically accelarated by CheZ phosphatase (*4, 12, 13*). This allows a fast reset of CheY-P levels to equilibrium in the absence of a tactic signal. Thus, signaling in *E. coli* manifests itself as a balance between the phosphorylated and the unphosphorylated state of the response regulator, CheY.

Certain features of motility and chemotaxis in the soil bacterium *Rhizobium meliloti* are distinctly different from those seen in *E. coli* (*14*−*16*). The free-swimming behavior of *R. meliloti* is directed by variations in flagellar rotary speed, rather than by switches between clockwise and counterclockwise rotation, as in *E. coli* (*17*). The chemotaxis signal transduction chain of *R. meliloti* contains, along with a CheA histidine kinase, two different response regulators, CheY1 and CheY2, but no homologue of CheZ phosphatase (*18*). In vivo analyses of the deletion mutants, Δ*cheA*,

†This work was supported by a grant from the Deutsche Forschungsgemeinschaft (Schm 68/24-2).

* To whom correspondence should be addressed. Tel: +49-941 9433162. Fax: +49-941 9433163. E-mail: Rudy.Schmitt@biologie.uni-regensburg.de.

[1] Abbreviations: 2YT, double yeast extract−tryptone; 3D, three-dimensional; AcP, acetyl phosphate; Ap^R, ampicillin-resistant; BSA, bovine serum albumin; CheY1-P, phospho-CheY1; CheY1-^{32}P, [^{32}P]-phospho-CheY1; CheY1I-P, phospho-CheY2; CheY2-^{32}P, [^{32}P]phospho-CheY2; ECL, enhanced chemiluminescence; EDTA, ethylenediaminetetraacetic acid; IPTG, isopropyl β-D-thiogalactopyranoside; kDa, kilodalton(s); Km^R, kanamycin-resistant; [^{32}P]AcP, acetyl [^{32}P]phosphate; PAGE, polyacrylamide gel electrophoresis; PBS, phosphate-buffered saline; P-CheA, phospho-CheA; ^{32}P-CheA, [^{32}P]phospho-CheA; P_i, inorganic phosphate; SDS, sodium dodecyl sulfate; Sm^R, streptomycin-resistant; $t_{1/2}$, a half-time of reaction; TBS-T, Tris-buffered saline−Tween; TEDG, Tris-EDTA−dithiotreitol−glycerol (buffer); TY, tryptone−yeast extract.

S0006-2960(97)02330-1 CCC: $15.00
Published on Web 02/07/1998

Table 1: Strains and Plasmids

strain/plasmid	markers[a]	source/ref
strain		
E. coli		
JM109	*recA1 endA1 gyrA96 thi hsdR17 relA1* Δ*(lac-proAB)* /F′ *traD36 proAB lacI*^{q} *lacZ DM15*	(*20*) cloning host
M15[pREP4]	Km^R Nal^S Sm^S rif^S lac$^-$ ara$^-$ gal$^-$ mtl$^-$ F$^-$ recA$^+$ uvr$^+$ pQE expression host	Qiagen
R. meliloti		
RU11/001	spontaneous Sm^R derivative of RU10/406, Che$^+$	(*21*)
RU11/307	Sm^R *cheY2*Δ	(*16*)
RU11/308	Sm^R *cheY1*Δ	(*16*)
RU11/309	Sm^R *cheY1*Δ/*cheY2*Δ	(*16*)
RU11/310	Sm^R *cheA*Δ	(*16*)
plasmid		
pJOE890	Ap^R	J. Altenbuchner
pUC18/19	Ap^R	(*22*)
pUCBM20	Ap^R	Boehringer Mannheim
pK18 *mob sacB*	Km^R *lacZ mob sacB*	(*23*)
pQE30	Ap^R, expression vector containing T5 promoter, N-terminal 6 × His tag	Qiagen
pQE60	Ap^R, expression vector containing T5 promoter, C-terminal 6 × His tag	Qiagen
pRU1221	Ap^R, Km^R, recombinant of 10.2-kb *Eco*RI chromosomal fragment containing *che* region of *R. meliloti* with Tn*5* insertion and pJOE890	(*18*)
pRU1224	Ap^R, recombinant of 3.1-kb *Sac*I chromosomal fragment of *R. meliloti* and pUC18	(*18*)
pRU1719	Ap^R, recombinant of 1.2-kb *Ksp*I fragment containing *cheY1* and pUCBM20	this work
pRU1722	Km^R, recombinant of PCR-generated 1.2-kb fragment containing *cheY1* with an Asp−53 to Glu exchange (CheY1D53E) and pK18*mob sacB* (*Ksp*I)	this work
pRU1735	Ap^R, recombinant of PCR-generated 0.4-kb fragment containing *cheY1* and pQE60 (*Nco*I/*Bgl*II)	this work
pRU1736	Ap^R, recombinant of PCR-generated 0.4-kb fragment containing *cheY2* and pQE60 (*Nco*I/*Bgl*II)	this work
pRU1737	Ap^R, recombinant of PCR-generated 0.4-kb fragment containing *cheY1D53E* and pQE60 (*Nco*I/*Bgl*II)	this work
pRU1742	Ap^R, recombinant of PCR-generated 2.3-kb fragment containing *cheA* and pQE30 (*Bam*HI/*Hin*dIII)	this work

[a] Nomenclature according to refs *24* and *25*.

Δ*cheY1*, and Δ*cheY2*, have shown that CheY2-P is the chief regulator of flagellar rotary speed and thereby mediates the tactic response (*16*). Deletion of *cheY1* had only a moderate effect on chemotaxis; however, it took this mutant considerably longer to adapt to the removal of attractant, a phenotype reminiscent of the behavior seen in *cheZ* mutants of *E. coli* (*19*).

We have previously postulated (*16*) that CheY1 accelerates adaptation to negative stimuli by regulating the level of CheY2-P. To elucidate the underlying mechanism, we have studied in vitro the phosphotransfer between the purified CheA, CheY1, and CheY2 proteins and the spontaneous dephosphorylation rates of CheY1-P and CheY2-P. Our findings led to a new mechanism for the signal transduction in *R. meliloti*, where the auxiliary response regulator, CheY1, acts as a phosphate sink in the three-component mixture, CheA/CheY1/CheY2. Accordingly, CheY1 assumes the role of the phosphatase required for quick adaptation in the *R. meliloti* signal transduction chain.

EXPERIMENTAL PROCEDURES

Bacterial Strains and Plasmids. Strains and plasmids used in this study are described in Table 1. *R. meliloti* was grown in TY medium (*26*). *E. coli* strains were grown in 2YT (1.6% Bacto tryptone, 1% yeast extract, 0.5% NaCl, pH 7.0).

DNA Methods. E. coli plasmid DNA was prepared according to Li and Schweizer (*27*). DNA was sequenced according to Sanger et al. (*28*) using the Quick Denature Sequenase kit (USB, Cleveland, OH) and ^{35}S-dATP (Amersham Buchler, Braunschweig, Germany).

Protein Purification. Recombinant proteins were expressed with a terminal 6× His affinity tag. C-Terminally tagged CheY1, CheY1D53E, and CheY2 and N-terminally tagged CheA were purified on Ni-NTA spin columns (Qiagen, Hilden, Germany) under native conditions as described by the manufacturer with the following modifications. Bacterial cultures were grown at 30 °C until OD_{600} reached 0.8 and expression was induced by the addition of 0.6 mM IPTG final concentration. Lysis, wash, and elution buffers were supplemented with 10% glycerol. Eluted proteins were dialyzed overnight against TEDG buffer (50 mM Tris, pH 7.9; 0.5 mM EDTA; 1 mM Dithiothreitol; 10% glycerol). Protein concentrations were determined (*42*) using the DC Protein Detection kit (BioRad, München, Germany) with BSA as a protein standard. Purity of the proteins was estimated from SDS−PAGE gels stained with Coomassie blue using ImageMaster Version 2.01 (Pharmacia Biotech, Freiburg, Germany). Purified proteins were stored in TEDG buffer at −20 °C. Protein activity was not affected by the storage of samples for at least 6 months.

Synthesis of Acetyl [^{32}P]Phosphate. Acetyl [^{32}P]phosphate was prepared according to Stadtman (*30*) with modifications described by McCleary and Stock (*31*). The acetyl phosphate was assayed spectrophotometrically using its ability to react with hydroxylamine at pH 6.5−7.0 to form hydroxamic acids, which in the presence of ferric salts produce red to violet complexes (*30*). Unlabeled acetyl phosphate (Sigma, Deisenhofen, Germany) was used as a standard.

Purification of [^{32}P]Phospho-CheA. Purified CheA (1.2 nmol) was phosphorylated in TEDG buffer (pH 7.9) in the presence of 0.4 mM [γ-^{32}P]ATP (∼800 cpm/pmol, Amersham Buchler), 5 mM $MgCl_2$, and 50 mM KCl at 20 °C for 10 min. [^{32}P]Phospho-CheA was purified from [γ-^{32}P]ATP using Nanosep 30K columns (Pall Filtron, Dreieich, Germany). Samples (200 μL) were concentrated by centrifugation at room temperature for 5 min and washed twice with 400 μL of ice-cold TEDG buffer. The purity of radiolabeled CheA was controlled by SDS−PAGE and autoradiography,

Scheme 1

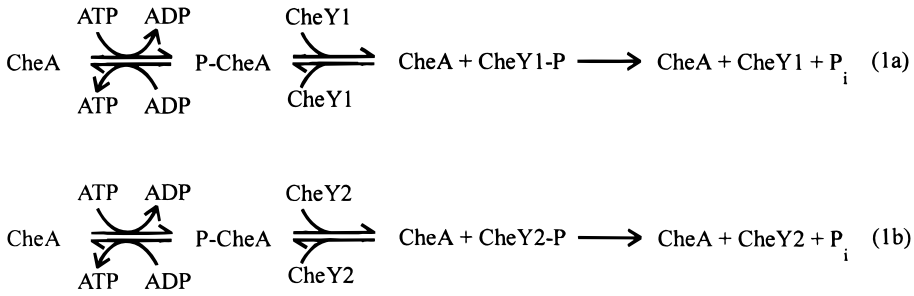

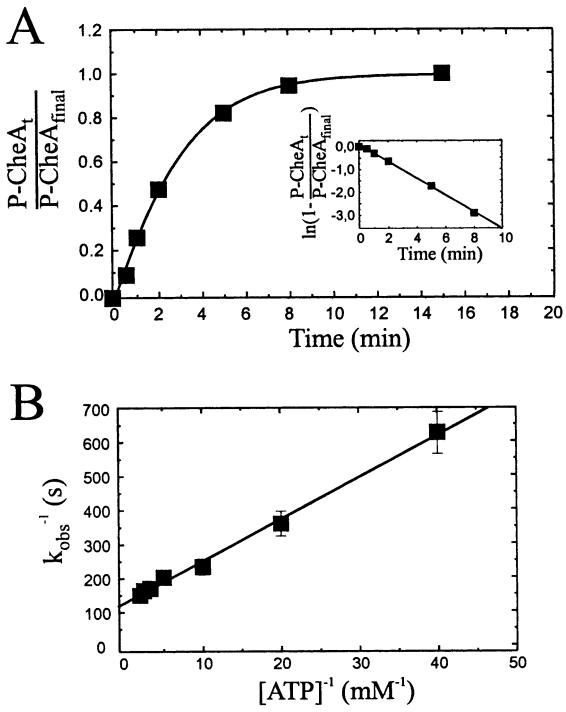

FIGURE 1: Kinetics of ATP-dependent autophosphorylation of CheA. (A) Time course of CheA phosphorylation. CheA (2 μM final concentration) was incubated with 0.4 mM [γ-^{32}P]ATP at 20 °C (see Experimental Procedures). Aliquots (10 μL) were withdrawn at specified intervals, the reaction was terminated by 5 μL of 3× SDS−PAGE sample buffer/EDTA, and the mixture was separated by SDS−PAGE. Following autoradiography, ^{32}P-CheA bands were excised and quantified by scintillation counting. The line through the experimental data points represents a computer-generated least-squares fit of the data to a single-exponential curve. A semilogarithmic plot of the determined time course is shown in the inset. (B) Double-reciprocal plot (Lineweaver−Burk plot) of the observed pseudo-first-order rate constant (k_{obs}) for CheA autophosphorylation versus ATP concentration. Error bars represent the standard errors of the mean of two experiments.

and the concentration of purified [^{32}P]phospho-CheA was determined by liquid scintillation counting of CheA bands excised from the gel (LS335 counter, Beckman Instruments, Palo Alto, CA). Under these conditions, the ratio [^{32}P]-phospho-CheA: CheA was 1:4.

Phosphorylation Assays. All phosphorylation reactions were performed in TEDG buffer, pH 7.9, supplemented with 5 mM $MgCl_2$ and 50 mM KCl at 20 °C. The concentration of proteins, ATP, and acetyl phosphate in each reaction and the reaction times are specified in the figure legends. Autophosphorylation of CheA, as well as transphosphorylation of CheY1 and CheY2 in the presence of CheA and ATP, was initiated by the addition of [γ-^{32}P]ATP (~800 cpm/pmol; 0.025−0.5 mM final concentration). Phosphotransfer reactions from purified ^{32}P-CheA to CheY1 and CheY2 were initiated by the addition of CheY1 or CheY2 to ^{32}P-CheA. CheY1-^{32}P and CheY2-^{32}P were prepared by the addition of acetyl [^{32}P]phosphate (~30 cpm/pmol; 7−18 mM final concentration) to purified CheY1 or CheY2 proteins. To determine the dephosphorylation rates of CheY1-P and CheY2-P, either 30 μM CheY1 or 30 μM CheY2 was phosphorylated by 7 mM acetyl [^{32}P]phosphate for 5 min and CheY1-^{32}P and CheY2-^{32}P were chased by adding unlabeled acetyl phosphate to 100 mM final concentration.

Phosphotransfer was measured by sampling (10-μL aliquots) the reaction mixture at specified intervals after the reaction was stopped by addition of 5 μL of 3× SDS−PAGE sample buffer that contained 10 mM EDTA. Samples were separated by electrophoresis on SDS-containing 7.5% or 15% polyacrylamide gels, and size was estimated by comparison with prestained SDS−PAGE standards (BioRad). Immediately following electrophoresis, gels were vacuum-dried and exposed on Kodak BioMax film. Following autoradiography, the radiolabeled bands were excised and quantified by liquid scintillation counting (LS335 counter, Beckman) or the intensity of bands on the film quantified by Image-Master Version 2.01 (Pharmacia Biotech).

Preparation of Cell Extracts from Chemotaxis-Proficient R. meliloti Cells. Approximately 10^9 cells of *R. meliloti* were starved in 100 mL of RB buffer (*15*) without a carbon source at 30 °C for 16 h, harvested, resuspended in TY to OD_{600} = 0.05, and grown at 30 °C for 4 h. Cells were collected, washed with 2 mL of PBS (80 mM Na_2HPO_4, 20 mM NaH_2PO_4, 100 mM NaCl, pH 7.5), resuspended in 1 mL of PBS, and frozen in ethanol/dry ice. After thawing, cells were sonicated on ice (100 W/10 min) and sedimented at 14000*g* (4 °C, 10 min). The supernatant was collected and its protein concentration determined.

Quantification of Western Blots. Aliquots of the supernatant fraction from motile cells (from 5 to 30 μg of protein) and from 5 to 50 ng of purified recombinant CheY1, CheY2, and CheA proteins were separated by 15% (CheY1 and CheY2) or 7.5% (CheA) SDS−PAGE. Gels were blotted onto a Hybond C membrane (Amersham Buchler) using a Trans-Blot SD semidry electrophoretic transfer cell (BioRad) at 15 V for 50 min with transfer buffer containing 0.0375% SDS as described by the manufacturer. Membranes were blocked with 5% blocking reagent in TBS-T buffer (20 mM Tris-HCl, 138 mM NaCl, 0.2% Tween 20) at room temperature for 1 h. Membranes were incubated with polyclonal rabbit antibody (1:1000 dilution in TBS-T) raised against *R. meliloti* CheY1, CheY2, and CheA proteins, respectively. The antisera were prepared by Eurogentec (Seraing, Belgium). After 1 h of incubation, membranes were washed

with TBS-T once for 15 min and then twice for 5 min. Bands were visualized by chemiluminescence using goat-anti-rabbit antibody (Sigma; 1:4000 dilution in TBS-T) complexed with peroxidase and the ECL detection kit (Amersham Buchler). Membranes were exposed on Fuji RX New film and quantified by ImageMaster Version 2.01 (Pharmacia Biotech). The concentrations of CheY1, CheY2, and CheA in cell extracts were calculated by comparison with defined amounts of the purified proteins run and blotted in parallel.

RESULTS

Kinetics of CheA Autophosphorylation. Recombinant *R. meliloti* CheA protein with an N-terminal 6× His affinity tag was overexpressed in *E. coli* and purified as described under Experimental Procedures. The purity of the protein was ≥90% as estimated from a SDS−PAGE gel. Purified CheA (2 μM) was incubated with [γ-^{32}P]ATP, its concentration varying from 0.025 to 0.5 mM. Aliquots were removed at specified intervals, the reactions were terminated by the addition to SDS−PAGE sample-loading buffer that contained 10 mM EDTA, and separation was carried out by SDS−PAGE. Similar to *E. coli*, the ATP-dependent autophosphorylation of *R. meliloti* CheA follows a simple exponential time course (Figure 1A). Pseudo-first-order rate constants (k_{obs}), determined from semilogarithmic plots of the reaction time courses (Figure 1A, inset), exhibited a hyperbolic dependence on the ATP concentration (not shown), such that a linear double-reciprocal plot of k_{obs}^{-1} versus $[ATP]^{-1}$ (Figure 1B) facilitated the definition of binding interactions between CheA and ATP and the autophosphorylation rate constant. In terms of a Michaelis−Menten equation, the apparent K_m value thus defined was 0.1 mM, close to the K_m value of 0.3 mM of the *E. coli* CheA (*6*). The limiting rate constant for the autophosphorylation of *R. meliloti* CheA, corresponding to V_{max}/[CheA], was determined to be approximately 0.008 s^{-1} at saturating ATP concentration.

CheA-Dependent Phosphorylation of CheY1 and CheY2 in the Presence of [γ-^{32}P]ATP. Recombinant CheY1 and CheY2 with a C-terminal 6× His affinity tag were overexpressed and purified as described under Experimental Procedures. The C-terminal 6× His tag fusion does not impair the phosphorylation and regulatory functions of the *E. coli* CheY (*32*), an observation that also applies to the CheY1 and CheY2 proteins of *R. meliloti*. These, upon elution from a Ni-NTA column, had an estimated purity of ≥99%. We first investigated the phosphorylation of CheY1 and CheY2 by the CheA kinase under multiple-turnover conditions that approximate those found intracellularly. Upon addition to a CheA/[γ-^{32}P]ATP mixture, both CheY1 and CheY2 were rapidly phosphorylated (Figure 2A,B), confirming that CheA is the cognate kinase for both of these response regulators. Neither CheY1 nor CheY2 was phosphorylated by ATP itself. By assuming that the phosphorylation reactions proceed similarly to those studied in *E. coli* (*7, 33*), the net equations for the phosphorylation of CheY1 and CheY2 can be schematically represented (Scheme 1).

The equilibrium for CheY phosphorylation by P-CheA in *E. coli* is shifted far toward the formation of CheY-P (*33*), but reverse phospho transfer from CheY-P to CheA has also been observed (*7, 34*).

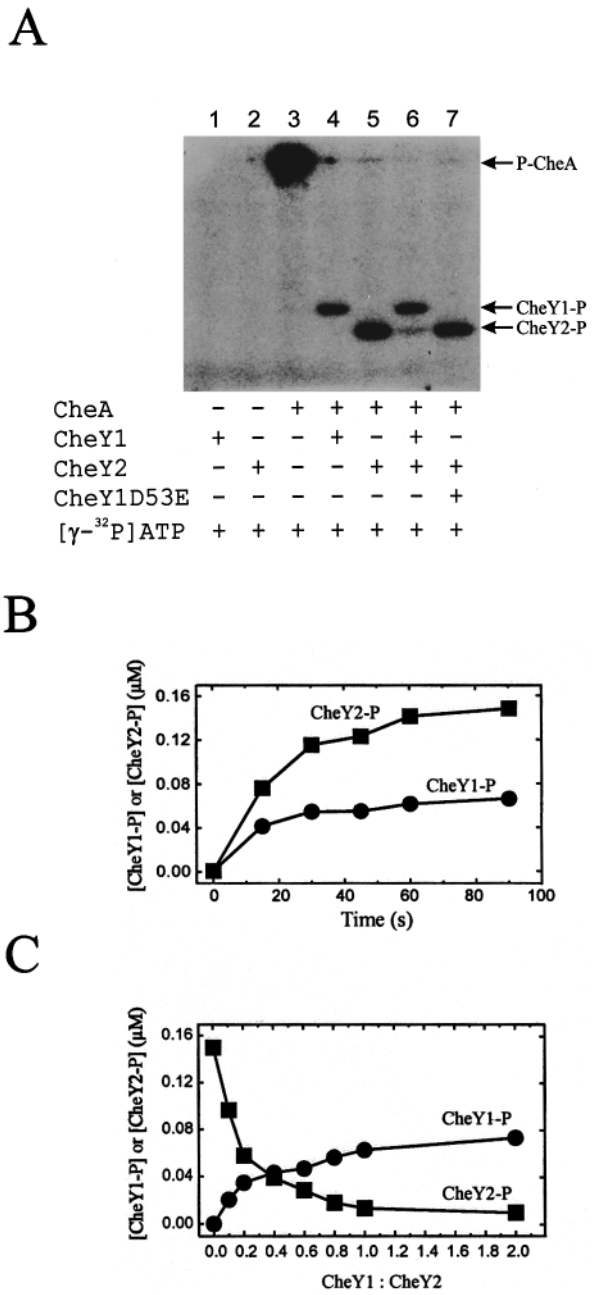

FIGURE 2: CheA-dependent phosphorylation of CheY1 and CheY2 in the presence of [γ-^{32}P]ATP. Reactions contained 5 μM CheA, 10 μM CheY1, 10 μM CheY1D53E, and 10 μM CheY2 in the indicated combinations. Samples were analyzed for phospho-CheA, phospho-CheY1, and phospho-CheY2 as described under Experimental Procedures. (A) Autoradiogram after separation of reactants by 15% SDS−PAGE. The presence (+) or absence (−) of reactants in each mixture is indicated below the lanes. The mixtures (10 μL final volume) were incubated with 0.4 mM [γ-^{32}P]ATP at 20 °C for 2 min and terminated by 5 μL of 3× SDS−PAGE sample buffer/EDTA. (B) Progress curves for the phosphorylation of CheY1 or CheY2 by P-CheA. At indicated times after [γ-^{32}P]ATP addition, 10-μL aliquots of the reaction mixture were sampled and terminated as in A and quantified by scintillation counting. (C) Dependence of CheY1 and CheY2 steady-state phosphorylation by CheA on the ratio of CheY1 to CheY2. CheA (5 μM final concentration) and CheY2 (10 μM final concentration) were incubated with varying amounts of CheY1 (0−20 μM) and 0.4 mM [γ-^{32}P]ATP at 20 °C for 2 min. Data points were determined as in B. Each data point represents the average of three independent experiments: (●) CheY1-P; (■) CheY2-P.

To simulate the in vivo situation, reactant concentrations close to those present in *E. coli* were used (*8, 35, 36*). Under

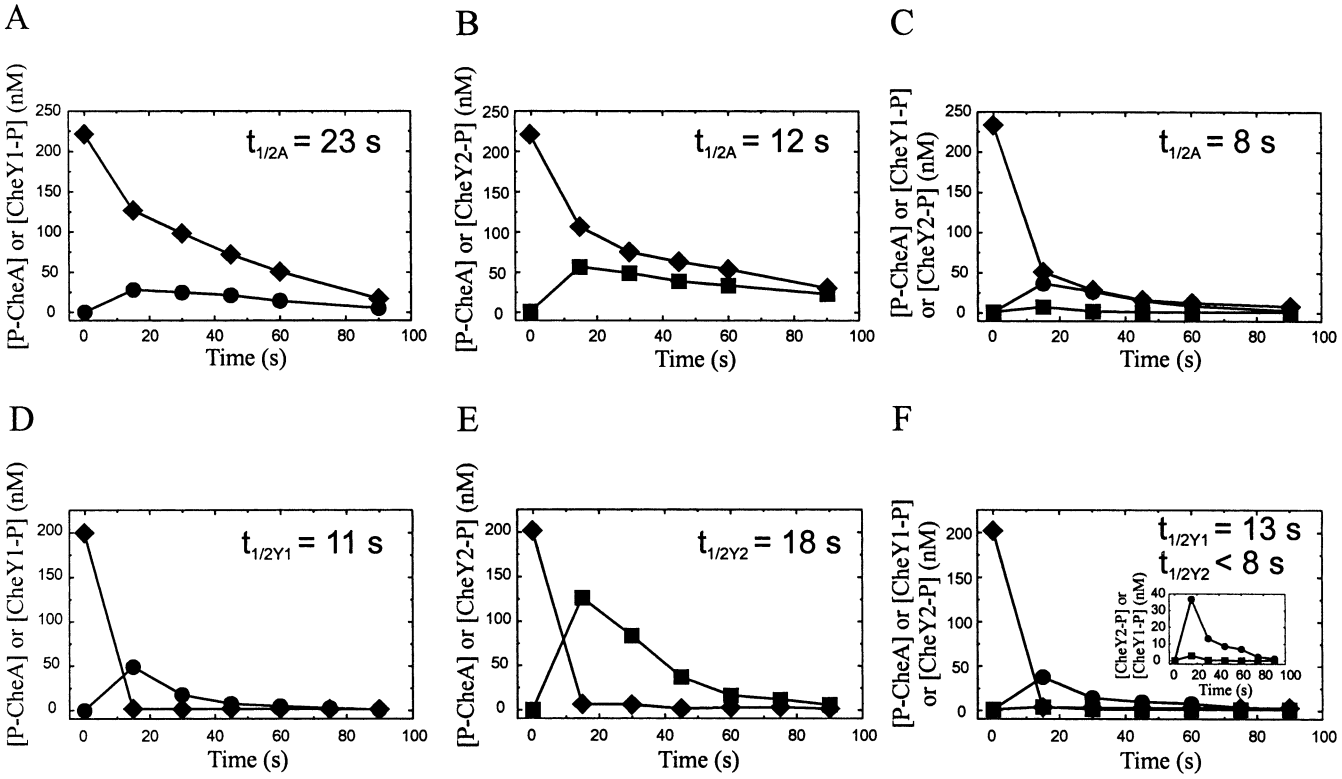

FIGURE 3: Phosphotransfer from ^{32}P-CheA to CheY1 and CheY2. ^{32}P-CheA was mixed with CheY1 and CheY2 as specified, and reactions were monitored as described under Experimental Procedures. Reactions contained the following: (A) 0.225 μM ^{32}P-CheA (initial concentration) and 0.6 μM CheY1; (B) 0.225 μM ^{32}P-CheA (initial concentration) and 0.6 μM CheY2; (C) 0.225 μM ^{32}P-CheA (initial concentration), 0.6 μM CheY1, and 0.6 μM CheY2; (D) 0.2 μM ^{32}P-CheA (initial concentration) and 2 μM CheY1; (E) 0.2 μM ^{32}P-CheA (initial concentration) and 2 μM CheY2; and (F) 0.2 μM ^{32}P-CheA (initial concentration), 2 μM CheY1, and 2 μM CheY2. Each data point represents the average of two independent experiments: (●) CheY1-P; (■) CheY2-P; and (◆) P-CheA. Apparent half-times of dephosphorylation reactions ($t_{1/2Y1}$, $t_{1/2Y2}$, $t_{1/2A}$; defined in text) were calculated using computer-generated least-squares fits of the data to single-exponential curves.

these conditions, using 5 μM CheA, 10 μM CheY1, 10 μM CheY2, and 0.4 mM [γ-^{32}P]ATP, the phosphorylation of CheY1 and CheY2 proceeded with a half-time of approximately 14 s (Figure 2B). At these concentrations, the generation of CheY1-P and CheY2-P was limited by the rate of CheA autophosphorylation (compare Figure 1A). The same conclusion was drawn from the disappearance of the ^{32}P-CheA band upon addition of CheY1 or CheY2 to the autophosphorylation reaction of CheA (Figure 2A, lanes 4 and 5). The steady-state level of CheY2-^{32}P observed upon extended incubation (>60 s) was 2.2 times higher than that of CheY1-^{32}P (Figure 2B). If the phosphorylation of CheA is the rate-limiting step, differences in the levels of phosphorylation could be explained by a shorter half-life of CheY1-P in reaction 1a.

When both CheY1 and CheY2 were added at equimolar amounts, only CheY1, but not CheY2, revealed significant phosphorylation (Figure 2A, lane 6). The level of CheY1-^{32}P was similar with and without CheY2 present. Since a phosphate-nonaccepting mutant protein, CheY1D53E (with an Asp-53 to Glu exchange in the phosphorylation site), had no noticeable influence on the phosphorylation of CheY2 (Figure 2A, lane 7), it is unlikely that CheY1 mediates dephosphorylation of CheY2-P by phosphatase-like catalysis (see also below). Rather, competitive phosphorylation of CheY1 may be responsible for the observed effect (Figure 2C).

Phosphotransfer between Purified ^{32}P-CheA, CheY1, and CheY2 in the Absence of ATP. The rates of dephosphorylation of P-CheA by CheY1 and CheY2 were compared by use of purified ^{32}P-CheA as the phosphate donor. At 3-fold concentrations of CheY1 and CheY2 relative to ^{32}P-CheA (0.6 μM CheY1, 0.6 μM CheY2, and 0.225 μM ^{32}P-CheA), dephosphorylation of ^{32}P-CheA proceeded at a measurable rate, the apparent half-time of ^{32}P-CheA dephosphorylation ($t_{1/2A}$) by CheY1 and CheY2 being 23 and 12 s, respectively (Figure 3A,B). If, however, CheY1 and CheY2 were added

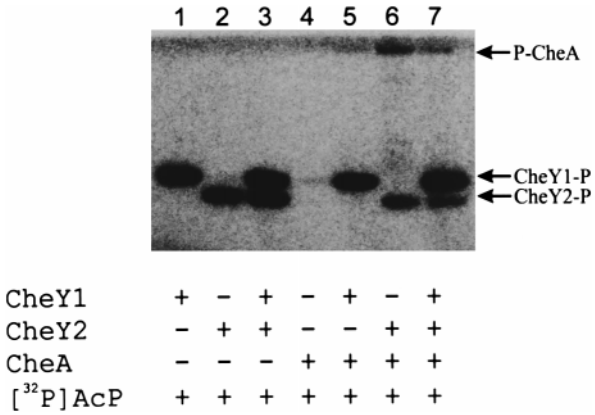

FIGURE 4: Phosphorylation of CheY1 and CheY2 by acetyl phosphate and phosphotransfer from CheY2-P to CheA. Reactions containing 7 μM CheY1 and/or 7 μM CheY2 were incubated with 18 mM acetyl [^{32}P]phosphate in 7 μL of reaction buffer for 60 s. Three microliters of either TEDG buffer (lanes 1, 2, 3) or CheA (final concentration 7 μM; lanes 4, 5, 6, 7) were added, and the reaction was stopped after a 20-s incubation by the addition of 5 μL of 3× SDS−PAGE sample buffer/EDTA. Samples were analyzed as described under Experimental Procedures.

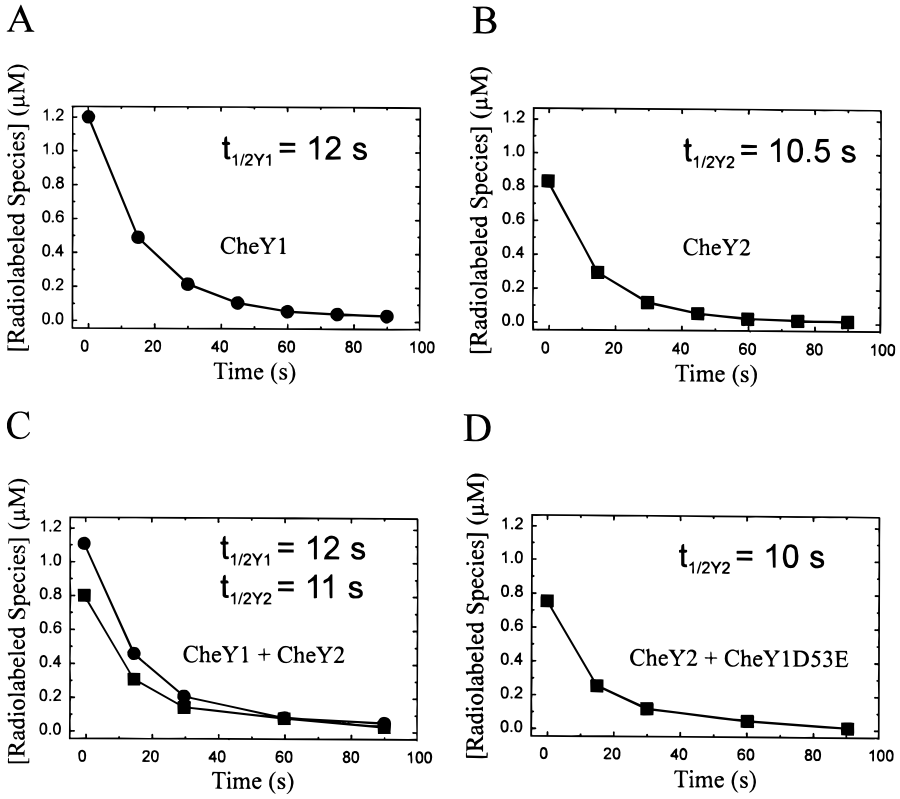

FIGURE 5: Time course of spontaneous dephosphorylation of CheY1-P and CheY2-P. CheY1 (30 μM) and CheY2 (30 μM) were phosphorylated with acetyl [^{32}P]phosphate and the dephosphorylation rate was measured by chasing CheY1-^{32}P and CheY2-^{32}P with excess unlabeled acetyl phosphate as described under Experimental Procedures. The dephosphorylation course of (A) CheY1-^{32}P; (B) CheY2-^{32}P; (C) CheY1-^{32}P and CheY2-^{32}P; and (D) CheY2-^{32}P in the presence of the phosphate-nonaccepting CheY1D53E mutant protein was defined. Each point represents the average of at least two independent experiments: (●) CheY1-^{32}P; (■) CheY2-^{32}P. Apparent half-times of dephosphorylation reactions ($t_{1/2Y1}$, $t_{1/2Y2}$) were calculated using computer-generated least-squares fits of the data to single-exponential curves.

together, the rate of ^{32}P-CheA dephosphorylation was distinctly higher (with an apparent half-time of 8 s), indicating phosphotransfer onto both CheY1 and CheY2 (Figure 3C). The dramatic decrease in CheY2-P as compared to CheY1-P (Figure 3C) thus reflects an accelerated degradation of CheY2-P in the three-component CheA/CheY1/CheY2 reaction, rather than the initial competition of CheY1 for phosphate. This was substantiated by the following observations.

If CheY1 or CheY2 was added at a 10-fold excess over ^{32}P-CheA (2 μM CheY1, 2 μM CheY2, and 0.2 μM ^{32}P-CheA), phosphotransfer to CheY1 and CheY2 was completed before the first sampling at 15 s, thus facilitating direct observations of the decay of CheY1-P and CheY2-P in the presence of unphosphorylated CheA (Figure 3D−F). The apparent half-time of CheY1-P decay in the presence of CheA $t_{1/2Y1}$ was 11 s; the decay of CheY2-P was slower ($t_{1/2Y2}$ = 18 s). This is consistent with the higher steady-state level of CheY2-P in reaction 1b. However, in the presence of both CheA and CheY1, the apparent half-time of CheY2-P decay $t_{1/2Y2}$ decreased to less than 8 s (Figure 3F, inset), whereas the rate of CheY1-P decay remained virtually unchanged ($t_{1/2Y1}$ = 13 s). Thus, in the presence of CheA, CheY2-P by itself is 1.7 times more stable than CheY1-P, whereas in the three-component system, CheA/CheY1/CheY2, the stability of CheY2-P is largely reduced. This result led us to examine the intrinsic turnover rates of the isolated phospho-CheY1 and phospho-CheY2 proteins.

Scheme 2

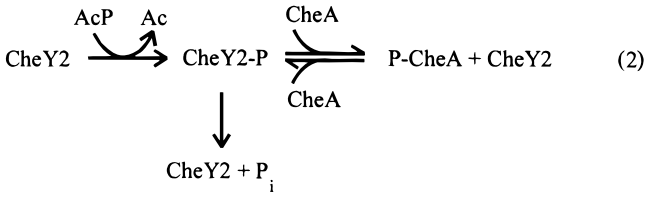

(2)

Phosphorylation of CheY1 and CheY2 by Acetyl Phosphate and the Reversed Phosphotransfer from CheY2-^{32}P to CheA. Studies by Lukat et al. (*12*) and McCleary and Stock (*31*) have demonstrated CheA-independent phosphorylation of CheY by acetyl phosphate. We have therefore synthesized and used acetyl [^{32}P]phosphate for the phosphorylation of CheY1 and CheY2 according to these authors (Figure 4, lanes 1 and 2). Under the given experimental conditions, steady-state levels of phosphorylated CheY1 and CheY2 were reached within 60 s (not shown).

Acetyl [^{32}P]phosphate did not phosphorylate CheA (Figure 4, lane 4). If, however, CheA was added to CheY2-^{32}P, reversed phospho transfer from CheY2-^{32}P to CheA was observed (Figure 4, lane 6) according to Scheme 2. By contrast, reversed phosphotransfer from CheY1-^{32}P to CheA was very low (Figure 4, lane 5). If in the same experiment CheY1 was added to the mixture of CheY2-^{32}P and CheA, a marked decrease in ^{32}P-CheA and CheY2-^{32}P band intensities and an increase in CheY1-^{32}P intensity were seen (Figure 4, lane 7). Although acetyl [^{32}P]phosphate was in excess, the apparent shift to CheY1-^{32}P phosphorylation suggested

that, in the three-component reaction, phosphotransfer from ^{32}P-CheA is strongly biased in favor of CheY1-^{32}P.

Dephosphorylation Rates of CheY1 and CheY2. The intrinsic rates of CheY1-^{32}P and CheY2-^{32}P decay (phosphate group turnover) in the absence of CheA were studied in a pulse-chase experiment with a 14-fold excess of unlabeled acetyl phosphate. The data presented in Figure 5 indicate apparent half-lives of 12 ± 1 s (CheY1-P) and 10.5 ± 1 s (CheY2-P). In view of these very similar spontaneous decay rates of CheY1-P and CheY2-P, it must be the equilibrium between P-CheA/CheY2 and CheA/CheY2-P given by eq 1b that causes the apparent higher stability of CheY2-^{32}P.

Does CheY1 dephosphorylate CheY2 by phosphatase-like activity? This possibility was examined by incubation of a mixture of CheY1-P and CheY2-P in the absence of CheA. Neither the steady-state level of CheY2-^{32}P (or CheY1-^{32}P) (Figure 4, lane 3) nor the dephosphorylation rates of CheY1-P or CheY2-P were affected (Figure 5C). Similarly, the phospho-nonaccepting mutant protein, CheY1D53E, had no accelerating effect on the dephosphorylation of CheY2-P (Figure 5D). This suggests that neither unphosphorylated CheY1 nor CheY1-P possesses phosphatase activity for hydrolyzing CheY2-P, assuming that the exchanged Asp-57 residue does not participate in the hypothetical phosphatase activity. This is rather unlikely, because in a mixture of CheY1-P and CheY2-P (Figure 4, lane 3) no such activity has been observed.

Quantification of in Vivo CheY1, CheY2, and CheA Concentrations. The in vivo concentrations of CheY1, CheY2, and CheA assessed by immunoblotting were matched with those used in vitro (Figure 6). In these experiments, varying volumes of cell extract (5−30 μg of protein) were compared to standardized amounts (5−50 ng) of purified CheY1 (Figure 6A), CheY2 (Figure 6B), and CheA (Figure 6C). Hybridizing bands were assigned to CheY1, CheY2, and CheA by their molecular sizes (CheY1, 14 kDa; CheY2, 14 kDa; CheA, 81 kDa) and by the hybridization patterns of extracts from three deletion mutants, Δ*cheY1*, Δ*cheY2*, and Δ*cheA* (Figure 6D−F). The His affinity tag was not immunogenic (data not shown). Band intensities were compared and quantified densitometrically. Approximate in vivo concentrations thus determined were CheA/CheY1/CheY2 as 1:13:13, corresponding to 850 (CheA)/11 000 (CheY1)/11 000 (CheY2) estimated number of molecules per cell or 1.5 μM CheA, 20 μM CheY1, and 20 μM CheY2 concentrations. The respective values for *E. coli* are 1 μM CheA to 15 μM CheY (*8*, *35*). The results confirm that protein concentrations used in the phosphotransfer experiments, namely, 0.2−30 μM CheA and 0.6−30 μM CheY1 and CheY2, were well in the range of those present in a chemotaxis-proficient *R. meliloti* cell.

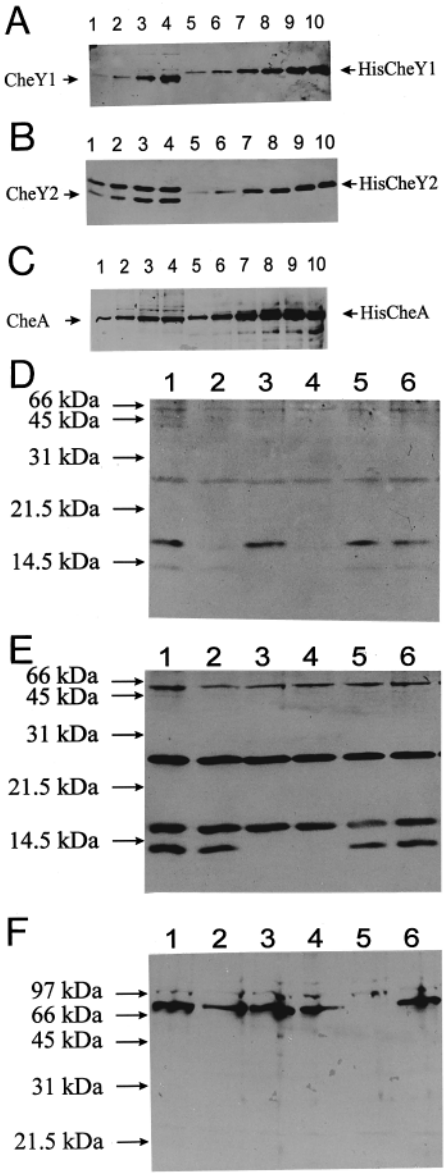

FIGURE 6: Determination of intracellular concentrations of CheY1, CheY2, and CheA by immunoblots. Soluble extracts of motile *R. meliloti* cells and purified CheY1, CheY2, and CheA proteins. Proteins and cell extracts were separated by either 15% (CheY1 and CheY2) or 7.5% (CheA) SDS−PAGE, blotted and hybridized as described under Experimental Procedures. (A, B, C) five (lane 1), 10 (lane 2), 20 (lane 3), and 30 μg (lane 4) of soluble extracts of *R. meliloti* RU11/001 (chemotaxis wild-type) and 5 (lane 5), 10 (lane 6), 20 (lane 7), 30 (lane 8), 40 (lane 9), and 50 ng (lane 10) of purified 6× His tagged proteins were hybridized against rabbit polyclonal (A) anti-CheY1, (B) anti-CheY2, and (C) anti-CheA antibody. (D, E, F) Twenty micrograms of soluble extract of *R. meliloti* RU11/001 (chemotaxis wild-type; lanes 1 and 6), RU11/308 (*DcheY1*; lane 2), RU11/307 (*DcheY2*; lane 3), RU11/309 (*DcheY1/DcheY2*; lane 4), and RU11/310 (*DcheA*; lane 5) were hybridized against rabbit polyclonal (D) anti-CheY1, (E) anti-CheY2, and (F) anti-CheA antibody. Molecular mass standards (BioRad) are indicated in kilodaltons. The 16-kDa band (B, lanes 1−4) represents a crossreacting protein other than CheY1, because this band is also present in a *cheY1* deletion mutant (E, lane 2).

DISCUSSION

We have analyzed in vitro the phosphotransfer between three key components, CheA, CheY1, and CheY2, of the *R. meliloti* chemotaxis signal transduction pathway. As in *E. coli*, CheA was shown to act as ATP-dependent autokinase capable of donating its phospho group to the response regulators, CheY1 and CheY2. These results confirmed previous assumptions based on mutant phenotypes (*16*). CheZ phosphatase that efficiently inactivates excessive free CheY-P in the *E. coli* system is absent from *R. meliloti*. This lack is compensated for by an additional CheY protein, CheY1, that controls the phosphorylation level of the main response regulator, CheY2-P. The in vitro studies reported here are summarized by the reaction scheme for the *R. meliloti* signal transduction (Scheme 3).

Scheme 3

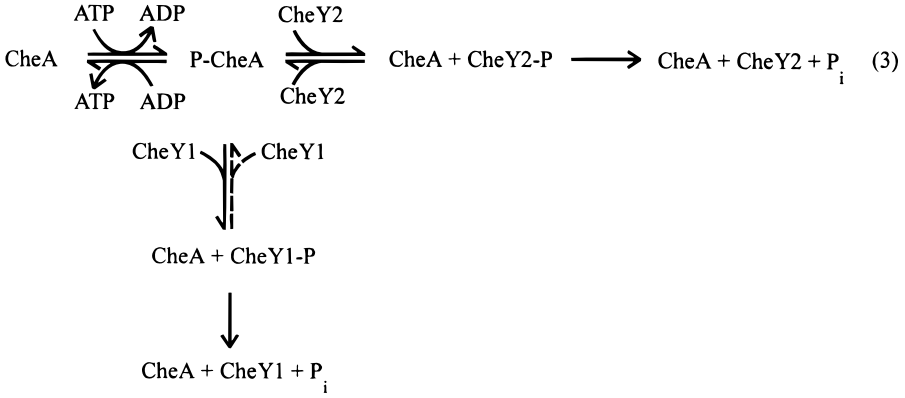

The scheme is consistent with the essential observations made in this study, namely: (i) CheA is an ATP-dependent autokinase; (ii) CheA phosphorylates both CheY1 and CheY2; (iii) phosphotransfer from CheA-P to CheY2 is reversible, and CheY2-P and CheA-P are in equilibrium, whereas phosphotransfer from CheY1-P to CheA appears to be insignificant (indicated by a dashed arrow); and (iv) CheY1-P and CheY2-P have intrinsic phosphatase activities and dephosphorylate at similar rates.

One important deviation from the *E. coli* chemotaxis signal transduction system is the observed regulatory role of reversed phosphotransfer between CheY2-P and CheA. A similar phosphotransfer from an acyl phosphate of the response regulator to a phosphoramidate of the histidine kinase in signal transduction has been implicated in other two-component systems (*37*, *38*). The phosphotransfer from the OmpR response regulator (aspartyl phosphate) to its cognate histidine kinase, EnvZ (phosphoramidate), has been shown in vitro in the *E. coli* osmotic sensory system (*39*), where it appears to play a physiological role in dephosphorylating phospho-OmpR. Phosphotransfer from aspartyl phosphate to a histidyl residue thus appears to be thermodynamically feasible. Studies of model compounds indicate that acyl phosphate should have the highest free energy of hydrolysis of any phosphorylated amino acid side chain (−10 to −13 kcal; *40*). Whereas this appears to be the case for the aspartyl phosphate of CheY2-P (capable of reversed phosphotransfer onto CheA), it is not true for the aspartyl phosphate of CheY1-P, which in this respect is similar to the *E. coli* CheY-P. It has been proposed (*41*) that this loss in high-energy state is compensated for by a conformational change in protein structure. A similar phosphorylation-activated conformational switch may be instrumental in CheY1-P of *R. meliloti*. Such conformational changes may be detectable by NMR, as has been shown by comparison of the structures of CheY and CheY-P from *E. coli* (*29*).

Associated with reverse phosphotransfer from CheY2-P to CheA is the competitive phosphorylation of two response regulators by one histidine kinase. The proposed model (eq 3) facilitates an answer to a principal problem of motion control and chemotaxis in *R. meliloti*: How, upon cessation of CheA activity, can an efficient termination of the CheY2-P control at the flagellar motor be accomplished without a CheZ-like phosphatase? As CheY2-P acts as chief regulator of the flagellar rotation rate (*16*), the balance between phosphorylated and unphosphorylated CheY2 is essential for adaptation. An intrinsic CheY2-P dephosphorylation with the half-time of 10.5 s is faster than that of *E. coli* CheY-P (20 s) but is too slow for efficient control of chemotaxis that requires exitation and adaptation in seconds or less (*43*). In vivo data have indicated that the level of CheY2-P is regulated by CheY1 (*16*). The phosphotransfer experiments reported here confirmed that CheY1 in conjunction with unphosphorylated CheA serves to quickly reduce the level of CheY2-P. Neither CheY1 nor CheA is a phosphatase of CheY2-P; their influence on CheY2-P levels is the result of shifting the equilibrium of reaction 3 toward the formation of CheY1-P. In *R. meliloti*, CheY1 thus assumes a dual role: (i) CheY1 competes for phosphate from P-CheA with an apparently higher affinity than CheY2 (Figure 2). Thereby CheY1 controls the phosphorylation of CheY2 in the response to tactic signals (up-regulation). (ii) CheY1 accelerates dephosphorylation of P-CheA and thereby the decay of CheY2-P, once the signal and, hence, the CheA autokinase activity are switched off (down-regulation). Under defined physiological concentrations (∼10 excess of CheY1 and CheY2 over CheA), CheY1 thus functions as a phosphate sink. It is reasonable to assume that in vivo the observed back-transfer of phosphate from CheY2 to CheY1 will be regulated by the CheW/receptor complex controlling CheA activity. This (along with "molecular crowding") may increase the rate constants up to 800-fold (*7*, *45*), a possibility that is currently being tested.

This type of regulation is new in two-component signal transduction pathways. However, the principle does not appear to be unique. Recent findings of two CheY homologues in *Rhodobacter sphaeroides* (*44*), *Caulobacter crescentus* (M. K. Alley, personal communication), and *Agrobacterium tumefaciens* (E. Wright, personal communication) suggest that the new reaction scheme may be a common feature in members of the α-subgroup of proteobacteria.

ACKNOWLEDGMENT

We thank Michael Eisenbach, Yuval Blat, and M. Germana Sanna for technical advice.

REFERENCES

1. Parkinson, J. S., and Kofoid, E. C. (1992) *Annu. Rev. Genet. 26*, 71−112.
2. Perego, M., and Hoch, J. A. (1996) *Trends Genet. 12*, 97−101.
3. Wolfe, A. J., Conley, P., Cramer, T. J., and Berg, H. C. (1987) *J. Bacteriol. 169*, 1878−1885.

4. Hess, J. F., Oosawa, K., Kaplan, N., and Simon, M. I. (1988) *Cell 53*, 79−87.
5. Bourret, R. B., Borkovich, K. A., and Simon, M. I. (1991) *Annu. Rev. Biochem. 60*, 401−441.
6. Tawa, P., and Stewart, R. C. (1994) *Biochemistry 33*, 7917−7924.
7. Stewart, R. C. (1997) *Biochemistry 36*, 2030−2040.
8. Ninfa, E. G., Stock, A., Mowbray, S., and Stock, J. (1991) *J. Biol. Chem. 266*, 9764−9770.
9. Sanders, D. A., Gillece-Castro, B. L., Stock, A. M., Burlingame, A. L., and Koshland, D. E, Jr. (1989) *J. Biol. Chem. 264*, 21770−21778.
10. Welch, M., Oosawa, K., Aizawa, S.-I., and Eisenbach, M. (1993) *Proc. Natl. Acad. Sci. U.S.A. 90*, 8787−8791.
11. Lukat, G. S., Lee, B. H., Mottonen, J. M., Stock, A. M., and Stock, J. B. (1991) *J. Biol. Chem. 266*, 8348−8354.
12. Lukat, G. S., McCleary, W. R., Stock, A. M., and Stock, J. B. (1992) *Proc. Natl. Acad. Sci. U.S.A. 89*, 718−722.
13. Blatt, Y., and Eisenbach, M. (1994) *Biochemistry 33*, 902−906.
14. Götz, R., and Schmitt, R. (1987) *J. Bacteriol. 169*, 3146−3150.
15. Götz, R., Limer, N., Ober, K., and Schmitt, R. (1982) *J. Gen. Microbiol. 128*, 789−798.
16. Sourjik, V., and Schmitt, R. (1996) *Mol. Microbiol. 22*, 427−436.
17. Platzer, J., Sterr, W., Hausmann, M., and Schmitt, R. (1997) *J. Bacteriol. 179*, 6391−6399.
18. Greck, M., Platzer, J., Sourjik, V., and Schmitt, R. (1995) *Mol. Microbiol. 15*, 989−1000.
19. Segall, J. E., Manson, M. D., and Berg, H. C. (1982) *Nature 296*, 855−857.
20. Yanish-Perron, C., Vieira, J., and Messing, J. (1985) *Gene 33*, 103−119.
21. Krupski, G., Götz, R., Ober, K., Pleier, E., and Schmitt, R. (1985) *J. Bacteriol. 162*, 361−366.
22. Vieira, J., and Messing, J. (1982) *Gene 19*, 259−268.
23. Schäfer, A., Tauch, A., Jäger, W., Kalinowski, J., Thiebach, G., and Pühler, A. (1994) *Gene 145*, 69−73.
24. Bachman, B. J. (1990) *Microbiol. Rev. 54*, 130−197.
25. Novick, R. P., Clowes, R. C., Cohen, S. N., Curtis, R., Datta, N., and Falkow, S. (1976) *Bacteriol. Rev. 40*, 168−189.
26. Beringer, J. E. (1974) *J. Gen. Microbiol. 84*, 188−198.
27. Li, M., and Schweizer, H. P. (1993) *Focus 14/15*, 19−20.
28. Sanger, F., Nicklen, S., and Coulson, A. R. (1977) *Proc. Natl. Acad. Sci. U.S.A. 74*, 5463−5467.
29. Lowry, D. F., Roth, A. F., Rupert, P. B., Dahlquist, F. W., Moy, F. J., Domaille, P. J., and Matsumura, P. (1994) *J. Biol. Chem. 269*, 26358−26362.
30. Stadtman, E. R. (1957) *Methods Enzymol. 3*, 228−231.
31. McCleary, W. R., and Stock, J. B. (1994) *J. Biol. Chem. 269*, 31567−31572.
32. Sanna, M. G., and Simon, M. I. (1996) *J. Biol. Chem. 271*, 7357−7361.
33. Hess, J. F., Bourret, R. B., and Simon, M. I. (1988) *Nature 336*, 139−143.
34. Garzon, A., and Parkinson, J. S. (1996) *J. Bacteriol. 178*, 6752−6758.
35. Stock, A., Koshland, D. E., Jr., and Stock, J. (1985) *Proc. Natl. Acad. Sci. U.S.A. 82*, 7989−7993.
36. Kuo, S. C., and Koshland, D. E., Jr. (1987) *J. Bacteriol. 169*, 1307−1314.
37. Hoch, J. A. (1995) in *Two-Component Signal Transduction* (Hoch, J. A., and Silhavy, T. J., Eds.) pp 129−144, ASM Press, Washington, DC.
38. Uhl, M. A., and Miller, J. F. (1996) *EMBO J. 15*, 1028−1036.
39. Dutta, R., and Inouye, M. (1996) *J. Biol. Chem. 271*, 1424−1429.
40. Jencks, W. P. (1980) *Adv. Enzymol. 51*, 75−106.
41. Stock, J. B., Surrete, M. G., Levit, M., and Park, P. (1995) in *Two-Component Signal Transduction* (Hoch, J. A., and Silhavy, T. J., Eds.) pp 25−51, ASM Press, Washington, DC.
42. Lowry, O. H., Rosenbrough, N. J., Farr, A. L., and Randal, R. J. (1951) *J. Biol. Chem. 193*, 265−275.
43. Stock, J. B., and Surette, M. G. (1996) *Escherichia coli and Salmonella typhimurium*: *Cellular and Molecular Biology*, 2nd ed., pp 1103−1129, ASM Press, Washington, DC.
44. Ward, M. J., Bell, A. W., Hamblin, P. A., Packer, H. L., and Armitage, J. P. (1995) *Mol. Microbiol. 17*, 357−366.
45. Borkovich, K. A., Kaplan, N., Hess, J. F., and Simon, M. I. (1989) *Proc. Natl. Acad. Sci. U.S.A. 86*, 1208−1212.

BI972330A